Electrically-Pumped Si-Laser Using Nano-Particle-Modified Metal-Oxide-Si Structures

Ching-Fuh Lin*, Eih-Zhe Liang, Chu-Ting Huang,
Kung-An Lin, and Shiu-Jia Shu
Graduate Institute of Electro-Optical Engineering
National Taiwan University
Taipei
TAIWAN
cflin@cc.ee.ntu.edu.tw

* also with Department of Electrical Engineering and
Graduate Institute of Electronics Engineering
Taipei
TAIWAN

***Abstract* – Measurement on the carrier lifetime shows that the radiative-recombination rate in Si can be enhanced to be more than twice of the non-radiative-recombination rate at large injection current using the nano-particle modified metal-oxide-silicon (MOS) structure. With the enhanced radiative recombination, the device with such a MOS structure exhibits lasing behaviours under forward bias of current injection at room-temperature and cw operation. The laser has the threshold current of 56 mA. The lasing wavelength well corresponds to the Si indirect-bandgap energy.**

I. INTRODUCTION

Si has been the most important material for electronics industry. Due to the mature technology of Si semiconductor, the IC market has grown tremendously over the past decades. However, the applications of Si in optoelectronics are still limited because it is incapable of producing light with good efficiency. Because Si is an indirect-bandgap semiconductor, it is very challenging to make Si efficiently emit light, particularly at its bandgap energy. Many efforts [1]-[4] have been devoted to breaking the limitation on light emission imposed by Si. They include porous-silicon-based devices [1], Si nano-crystals [2] and Raman lasers using Si [3]. Optical gain and Raman lasers on Si are achieved only with optical pumping. In addition, most of the past works have no results of light emission related to Si bandgap. In this work, we report the breakthrough of making lasers from Si at the Si indirect bandgap energy by electrical pumping using the nano-particle modified metal-oxide-silicon (MOS) structure.

II. POSSIBILITY OF ENHANCING LIGHT EMISSION AT THE INDIRECT-BANDGAP ENERGY

The main reason that hinders efficient light emission from Si is the low radiative recombination rate as a result of momentum mismatch between electrons and holes in Si. Therefore the non-radiative process can easily dominate the electron-hole recombination in Si. To make light emission from Si feasible, one has to solve two major problems. The first is to reduce the non-radiative recombination rate, so the radiative recombination can possibly dominate. The second one is to overcome the momentum mismatch between electrons and holes.

The measured minority carrier lifetime shows variation approximately from 10 μs to 1 ms, depending on the wafer quality. It means that the non-radiative recombination rate can be reduced for two orders of magnitudes if the Si-wafer has very good quality. Fortunately, the float-zone (FZ) wafers could have the minority carrier lifetime as long as 1ms, giving promise to the reduction of non-radiative recombination.

In addition, we had measured the minority carrier lifetime of MOS tunnelling diodes under forward bias. We discovered that the carrier lifetime highly depend on the injection current, indicating that radiative recombination rate increases with the injection current. Small-signal frequency response of the emitted light is used to monitor the lifetime in electroluminescent MOS tunnelling diodes. The light emission at the wavelength around 1.15 μm corresponds to the silicon band-edge electroluminescence (EL) and is characterized as phonon assisted band-to-band exciton recombination in silicon. This frequency response gives the information of minority carrier lifetime. In analysis of lifetime vs. bias current relation, non-radiative recombination and radiative recombination rates could be characterized. The carrier dynamics in the semiconductors is governed by the following rate equation:

$$\frac{d\delta p}{dt} = \frac{\eta_{inj} J}{ed} - (A + Bn + Cn^2)\delta p \qquad (1)$$

where δp is minority carrier density, n is majority carrier density, A is the coefficient of the Shockley–Read–Hall (SRH) recombination through the states near the Si/SiO_2 interface, B and C are radiative recombination and Auger recombination coefficients respectively, J is injection current density, η_{inj} is the minority carrier injection efficiency and d is effective accumulation depth. Rate equation (1) has frequency response (amplitude-frequency plot) proportional to $1/\sqrt{1+(2\pi f\tau)}$, where τ is the carrier lifetime and defined as $\tau=1/(A+Bn+Cn^2)$.

The minority carrier lifetime is influenced by the SRH recombination, electron-hole radiative recombination, and Auger recombination. Only the latter two factors lead to the dependence of lifetime on the carrier concentration, which is a function of the injection current. The measured variation of the carrier lifetime with the injection current is shown in Fig. 1 for three devices. Fig. 1 indicates that SRH recombination becomes less important for electroluminescent MOS tunnelling diodes as the injection current increases, compared to usual Si electronic devices. The curves in Fig. 1 show that the lifetime is inversely proportional to the injection current for low current density. Because the carrier density is

0-7803-9252-3/05/$20.00 ©2005 IEEE

approximately proportional to the injection current for sufficiently large biased voltage [5], the lifetime is inversely proportional to carrier density. The measurement shows that the Auger recombination is not obvious in this regime. With high level current injection (>3A/cm^2), the electroluminescent MOS tunnelling diode is operated in strong accumulation and the Fermi level is above the conduction band. Further injection of majority carriers (electron in n-type silicon) mainly makes accumulation depth extend deeper into silicon, rather than lifts up Fermi level. This means that majority carrier density n becomes less related to injection current. Consequently, lifetime becomes less dependent on injection current. Even so, the majority carrier density n can reach the order of 10^{19}~10^{20}cm^{-3}. On the other hand, the saturation of carrier density prohibits Auger recombination from playing an important role because Auger recombination is only significant at very large carrier density.

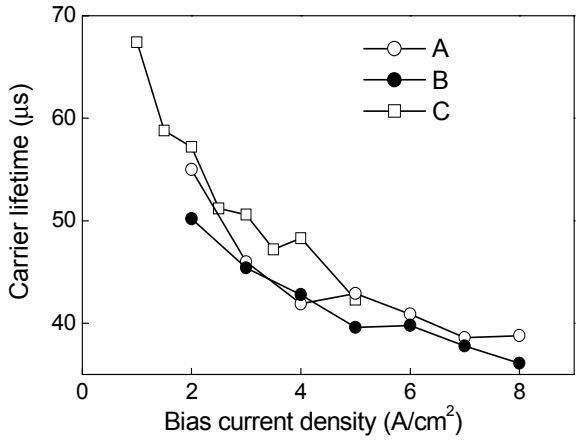

Fig. 1. Measured lifetime of different electroluminescent MOS tunnelling diodes A, B, and C.

For the above three devices, the external efficiency of light emission η_{ext} is 5x10^{-6}, 2x10^{-6} and 10^{-5} (W/A) respectively. With the same light extraction efficiency η_c and minority carrier injection efficiency η_{inj}, the external efficiency is proportional to radiative recombination efficiency η_{rec}, so $\eta_{ext}=\eta_c\eta_{inj}\eta_{rec}$. Under low level bias current density, lifetime is mainly governed by SRH recombination. The longer lifetime means less non-radiative recombination rate, so devices with longer lifetime could have better efficiency of light emission. Under high level bias current, the three devices have almost the same lifetime. It suggests that lowering lifetime at higher current density come from the increase of the radiative recombination rate.

The recombination coefficient, defined as the inverse of the lifetime, is plotted against the injection current density in Fig. 2. Because the Auger recombination is still not significant, the recombination coefficient can be described as $\tau^{-1} = A + Bn$. In addition, considering the saturation of the carrier density at strong accumulation, using the n-J relation as $n = \beta J/(1+\gamma J)$ gives a good fit to the experimental data in Fig.2. Then the recombination coefficient is related to the injection current density by $\tau^{-1} = A + B\beta J/(1+\gamma J)$, as shown by solid line in Fig. 2. From the curve fitting, we can identify individual contribution of radiative and non-radiative recombination rates. The A coefficient is 15539 sec^{-1}, ($B\beta$) is 4362 cm^{2}A^{-1}sec^{-1}, and $\gamma$is 0.06588cm^{2}A^{-1}.

Fig 2 shows that the recombination rate increases to almost three times as the injection current density increases from zero to 20 A/cm^2. The radiative recombination rate reaches 37645 sec^{-1}, more than twice of the non-radiative recombination rate. Ratio of radiative recombination rate to overall recombination rate, defined as radiative recombination efficiency η_{rec},

$$\eta_{rec} = Bn/(A+Bn) \qquad (2)$$

can be obtained, as shown by the dash line in Fig. 2. This ratio is more than 50% as the injection current density is larger than 5A/cm^2 and approaches 70 % at large injection current density. It indicates that radiative recombination is more efficient than non-radiative recombination, so efficient band-edge light emission from Si is possible.

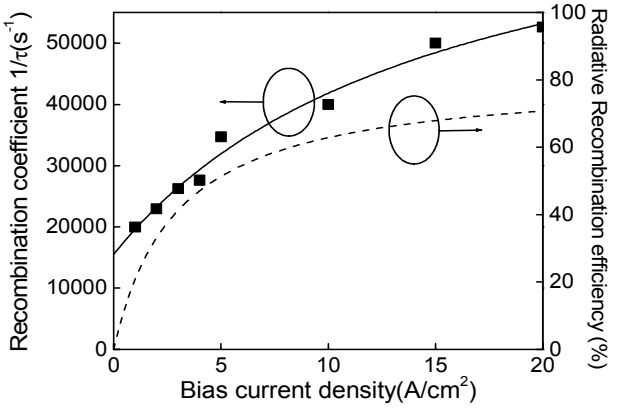

Fig. 2. Recombination coefficient vs. injection current density. (square dots: measured data; solid line: fitted curve using formula $\tau^{-1} = A + B\beta J/(1+\gamma J)$; dash line: radiative recombination efficiency estimated from the solid line.)

The A coefficient for Fig. 2 corresponds to the lifetime of only 64 μs. It is mainly governed by SRH recombination that will reduce the radiative recombination. The short lifetime indicates that the devices used for the above measurement do not have good enough quality. As mentioned before, the wafer with good quality can have the carrier lifetime as long as 1 ms, so the A coefficient can be reduced to only 1000 sec^{-1}. It will lead to nearly 100% of radiative recombination efficiency even at the low current density of 5A/cm^2. However, it is difficult to maintain the good quality at the Si surface that is particularly important for light emission from the MOS structure. Fortunately, the above measurement shows that even with the short lifetime of 64 μs, radiative recombination could dominate over the nonradiative recombination rate.

In addition to the consideration of carrier lifetime, it is also important to overcome the momentum mismatch between electrons and holes in Si. To have the momentum conservation, a phonon has to participate in the

recombination of an electron and a hole. The phonon provides the extra momentum equal to the momentum difference between the electron and the hole. It then makes the recombination behave like a three-particle process, leading to the low radiative recombination rate. If somehow the radiative recombination is modified to a two-particle process, the radiative recombination rate can be increased. We envision a process for this modification. The process is schematically shown in Fig. 3. First, an electron and a hole are confined within a limited region, so they will not freely move around. They either form an electron-hole pair or an exciton, thus behaving like a single particle. However, they still do not directly recombine because the momentum is not conserved. Then this particle-like electron-hole pair or exciton dissembles to emit a photon and a phonon. The emitted phonon has the momentum equal to the momentum difference between the electron and the hole.

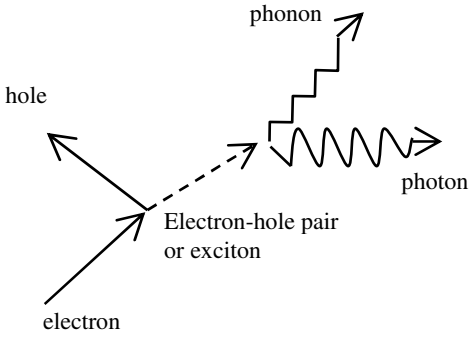

Fig. 3 Schematic of electron-hole recombination process for increasing radiative recombination rate.

To make electrons and holes spatially confined in a tiny region to prevent them from freely moving around, we use SiO_2 nanoparticles in the insulation layer of the MOS structure. Then when the MOS structure is under forward bias, a potential well with around 10-nm scale is established to confine one type of carriers. The other type of carrier also has much higher probability to tunnel through the MOS structure in the same region at the 10-nm scale than other regions. Therefore, electrons and holes are forced to form electron- hole pairs or excitons and the radiative recombination can be enhanced. The above measurement of radiative- recombination rate increased to be more than twice of the non-radiative-recombination rate is based on such a nano-particle modified MOS structure.

III. NANO-PARTICLE MODIFIED MOS STRUCTURE FOR ACHIEVING LASING FROM SILICON

A. Device Structure and Fabrication

The device is fabricated on N-type FZ Si substrate. The substrate was first cleaned with the standard procedure and spun on the solution containing SiO_2 nanoparticles with the size about 8-12 nm in diameter. The sample was then soft-baked to remove the solvent. Afterwards, a layer of 200-nm thick Al was evaporated onto the back side (without SiO_2 nanoparticles) of the wafer to form the bottom electrical contact. Before the top electrical contact was formed, the sample was placed in the atmosphere for five days. Because the spun SiO_2 nanoparticles are not tightly packed, oxygen molecules and water vapor in the air are able to reach the Si substrate that has no direct contact with the SiO_2 nanoparticles. Therefore, a thin layer of oxide was formed there. Then silver paint was applied on top of the SiO_2-nanoparticle layer to form the top electrical contact. The silver paint covers approximately a circular area with the diameter of 0.45 mm. A gold wire was connected to the silver paint before the paint was dried. The SEM cross section of a device with the nano-particle modified MOS structure is shown in Fig. 4. It shows that the individual SiO_2 nanoparticle has a size around 10 nm.

The layer of the SiO_2 nanoparticles is about 100 nm thick and should provide electrical insulation between the silver paint and the Si substrate. However, after the device was forward-biased for a while, the silver atoms were pulled through the hollow spaces between those particles and eventually formed nano-wires to reach the thin oxide on the Si surface. Therefore, the device behaves like a MOS tunneling diode.

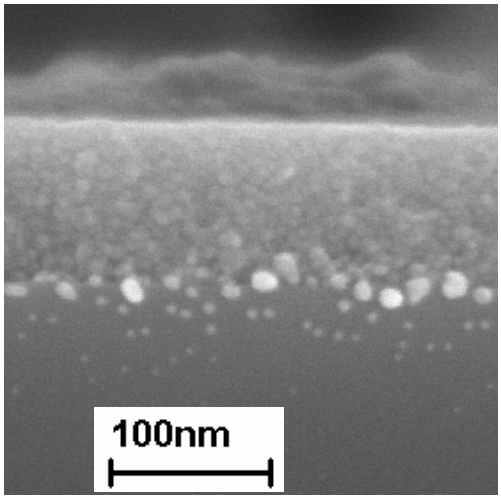

Fig. 4 A high-resolution SEM of the device cross section, consisting of three layers: Si substrate, SiO_2 nanoparticles and the top silver-paint layer.

B. Device Characteristics

At the Si/SiO_2 interface under the silver-paint area, the current flows only through the region that silver nano-wires touch the thin native oxide, while the other regions are blocked by the SiO_2 nanoparticles. This leads to two effects. First, in the forward bias, the thin-oxide regions touched by the silver nano-wires have a stronger voltage gradient than other regions. Thus the band bending of Si toward the thin-oxide regions is more severe than other regions, resulting in three-dimensional potential wells for electron confinement in the accumulation layer. Secondly, significant holes could tunnel through the region with very thin oxide from the silver to Si, while very negligible holes tunnel through the regions blocked by SiO_2 nanoparticles. This is equivalent to providing two-dimensional confinement for the tunnelled holes. Therefore, electrons and holes coincidentally

have the similar spatial confinement near the Si/SiO_2 interface. Such spatial confinement then leads to the easy formation of excitons or electron-hole pairs, so phonons are more easily involved in the electron-hole radiative recombination to overcome the momentum mismatch in the indirect-bandgap material. As a result, the region with the three-dimensional potential wells could provide optical gain for light amplification under electrical pumping.

In general, the devices with the MOS structure modified by the SiO_2 nanoparticles have the external quantum efficiency two orders of magnitudes higher than those just with the MOS structure without using SiO_2 nanoparticles. The nano-particle modified MOS structure could often have the external quantum efficiency near or above 10^{-4}. Please note that the MOS structure has the silver-paint pad blocks most of the light, so only light escaping from the peripheral of the pad is measured. Thus the measurable light is a very small portion of the radiative recombination. Fig. 5 shows a device emitting 10 μW of the output light at the Si bandgap energy. The external quantum efficiency is more than 10^{-4} even at the low injection current of 20 mA.

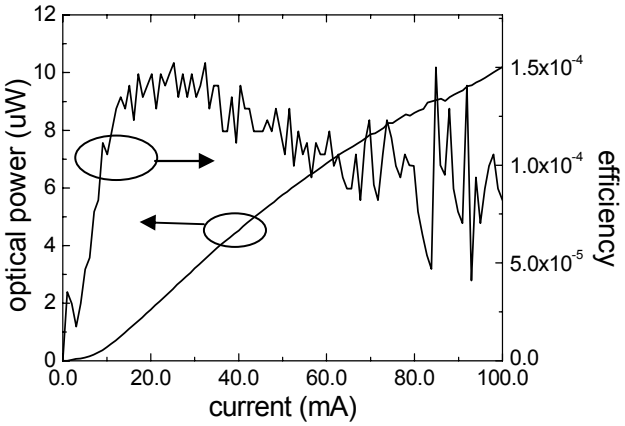

Fig. 5 L-I curve and external quantum efficiency of the nano-particle modified MOS light emitting diode.

With the enhanced radiative radiation, even lasing is obtained. The measured L-I curve of the lasing device is shown in Fig. 6. The device has an obvious threshold at 56 mA, corresponding to the current density of only 28.5 A/cm^2. The spectra of the emitted light at different current levels were measured and shown in Fig. 7. The emission wavelength is at the Si bandgap energy, corresponding to the wavelength of around 1150 nm. Below the threshold current, only spontaneous emission occurs, so the spectrum shows no emission spikes. Due to the band-filling effect, the emission spectrum covers a spectral range with the full width at half maximum (FWHM) of about 120 nm. Above the threshold, the spectra exhibit emission spikes, demonstrating particular enhancement of emissions at certain wavelengths due to the light amplification by the stimulated emission. The overall spectral range does not get further broadened at the high injection current. All of the measurements are under room temperature and cw operation. The measurements have been repeated for many times over several weeks and all show very similar results.

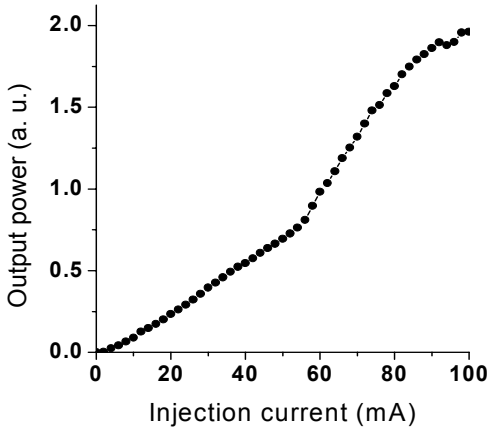

Fig. 6. L-I curve of the lasing device, showing the threshold at 56 mA and different differential quantum efficiencies below and above the threshold.

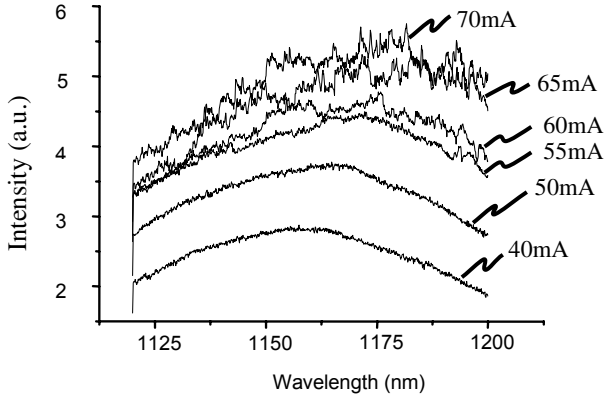

Fig. 7. Emission spectra at different current levels.

Different from light amplification in the direct-bandgap material that has the direct recombination of electrons and holes, the lasing behaviour in this device is caused by the involvement of phonon in the light-amplification process. The process is called as phonon-assisted stimulated emission. Such a process in Si is similar to the stimulated Raman scattering because both simultaneously generate one photon and one phonon. However, for phonon-assisted stimulated emission in Si, an exciton or an electron-hole pair transfers its energy to a photon and a phonon, but the stimulated Raman scattering involves no energy transfer from excitons or electron-hole pairs.

IV. CONCLUSION

Using nanoparticle-modified MOS structure, this work demonstrates electrically pumped lasing actions from Si under room-temperature and cw operation. The laser has the threshold current of 56 mA. The lasing wavelength well corresponds to the Si indirect-bandgap energy. Because the SiO_2 nanoparticles are used outside of the Si crystal, this scheme can be easily adapted to other indirect-bandgap materials like Ge, SiGe, AlAs, and SiC, etc. to generate

various wavelengths, including optical-fiber communication, visible, and ultraviolet regimes, for different applications.

V. ACKNOWLEDGMENT

This work is supported in part by the National Science Council, Taiwan, under the project numbers NSC 94-2112 -M-002-009 and NSC 94-2120-M-002-010.

VI. REFERENCES

[l] A. G. Cullis and L. T. Canham, "Visible light emission due to quantum size effects in highly porous crystalline silicon," *Nature* 353, 1991, pp. 335-338.

[2] L. Pavesi, L. Dal Negro, C. Mazzoleni, G. Franz, and F. Priolo, "Optical gain in silicon nanocrystals," *Nature* 408, 2000, pp.440-444.

[3] Haisheng Rong, Richard Jones, Ansheng Liu, Oded Cohen, Dani Hak, Alexander Fang, and Mario Paniccla, "A continuous-wave Raman silicon laser," *Nature*, 433, 2005, pp. 725-728.

[4] Ching-Fuh Lin, Peng-Fei Chung, Miin-Jang Chen, and Wei-Fang Su, Nanoparticle-modified metal–oxide–silicon structure enhancing silicon band-edge electroluminescence to near-lasing action, *Opt. Lett.* 27, 2002, pp. 713-715.

[5] Miin-Jang Chen, Ching-Fuh Lin, M. H. Lee, S. T. Chang and C. W. Liu, Carrier lifetime measurement on electroluminescent metal–oxide–silicon tunnelling diodes, *Appl. Phys. Lett.* 79, 2001, pp. 2264-2266.